POLİTEKNİK DERGİSİ

JOURNAL of POLYTECHNIC

ISSN: 1302-0900 (PRINT), ISSN: 2147-9429 (ONLINE)
URL: http://dergipark.org.tr/politeknik

Integration of solar panels in aircraft: evaluation of energy efficiency and aerodynamic performance

Model uçaklarda güneş panellerinin entegrasyonu: enerji verimliliği ve aerodinamik performansın değerlendirilmesi

***Yazar(lar) (Author(s))**: Cüneyd DEMİR[1], Merdin DANIŞMAZ[2], Ahmet KÖROĞLU[3]*

ORCID[1]: 0000-0002-4628-7786

ORCID[2]: 0000-0003-2077-9237

ORCID[3]: 0000-0002-1440-276X

To cite to this article: Demir C., Danışmaz M. and Köroğlu A., "Integration of Solar Panels In Aircraft: Evaluation of Energy Efficiency and Aerodynamic Performance", ***Journal of Polytechnic***, 29(4):290405:1-13 (2026).

Bu makaleye şu şekilde atıfta bulunabilirsiniz: Demir C., Danışmaz M. ve Köroğlu A., "Integration of Solar Panels In Aircraft: Evaluation of Energy Efficiency and Aerodynamic Performance", ***Politeknik Dergisi***, 29(4):290405:1-13 (2026).

Erişim linki (To link to this article): http://dergipark.org.tr/politeknik/archive

DOI: 10.2339/politeknik.1660926

Integration of Solar Panels in Aircraft: Evaluation of Energy Efficiency and Aerodynamic Performance

Highlights

- *The research successfully integrates solar panel cells into an aircraft design.*
- *Aerodynamic testing across various flight speeds with detailed analysis of drag and lift force.*
- *A novel aircraft design integrating renewable energy for improved energy efficiency.*

Graphical Abstract

This study examines the design and application of a solar-powered aircraft, with solar panels on its wings providing 15% of the required energy and improving performance across different speeds.

Figure. Aircraft featuring solar panel cells on its wings – illustration and actual

Aim

The objective of this study is to investigate the effectiveness of solar energy panels as a supplementary power source for a novel aircraft design, with the aim of assessing the aircraft's flight performance under various speed conditions.

Design & Methodology

The methodology adopted for this research comprises a design-based study focusing on a prototype aircraft with specified dimensions (2.5 m wingspan, 1.4 m length, and 0.5 m width) and a NACA 2412 airfoil. Data collection was carried out through aerodynamic testing at various flight speeds (1, 5, 10, 13, and 20 m/s), including measurements of aerodynamic forces, torque values, and energy contribution from solar panels.

Originality

This study contributes to the literature by integrating solar energy with flight mechanics, highlighting the potential of renewables in aviation and their impact on future aircraft design and sustainable aviation practices.

Findings

This research highlights practical and theoretical implications for aeronautical engineering and renewable energy, focusing on sustainable aircraft design, energy-efficient flight operations, and innovation in aviation materials

Conclusion

The results show that solar panels provided 15% of the flight energy, with a maximum lift force of 10.68 N at 20 m/s. As speed increased, both drag and lift increased, but drag rose 25% less than lift above 10 m/s. The discussion analyzes these findings in the context of aerodynamic theory, considering the optimal angle of attack, performance implications, and environmental effects on solar efficiency.

Declaration of Ethical Standards

The author(s) of this article declare that the materials and methods used in this study do not require ethical committee permission and/or legal-special permission.

Integration of Solar Panels in Aircraft: Evaluation of Energy Efficiency and Aerodynamic Performance

Araştırma Makalesi / Research Article

Cüneyd DEMİR[1*], Merdin DANIŞMAZ[2], Ahmet KÖROĞLU[3]

[1]Mucur Vocational School, Department of Computer Technologies, Kırşehir Ahi Evran University, Türkiye
[2]Faculty of Engineering and Architecture, Department of Mechanical Engineering, Kırşehir Ahi Evran University, Türkiye
[3]Mucur Vocational School, Department of Transportation Services, Kırşehir Ahi Evran University, Türkiye

(Geliş/Received : 02.10.2016 ; Kabul/Accepted : 26.08.2017 ; Erken Görünüm/Early View : 29.04.2025)

ABSTRACT

This study presents a case analysis involving the design and practical application of an aircraft featuring solar panel cells on its wings. The objective is to harness a portion of the energy required for flight from a renewable energy source, namely solar energy. The research evaluates the effectiveness of solar cells in an innovative aircraft design and assesses the aircraft's flight performance under various speed conditions. The prototype aircraft is designed with a wingspan of 2.5 m, a length of 1.4 m, and a width of 0.5 m, utilizing a NACA 2412 airfoil. Aerodynamic tests conducted at different flight speeds (1, 5, 10, 13, and 20 m/s) measured aerodynamic forces, torque values, and the energy contribution from the solar panels. The results indicate that the solar panels provide 15% of the energy required for flight, with a maximum lift force of 10.68 N achieved at 20 m/s. As flight speed increases, both drag and lift forces rise, with the rate of increase in drag being 25% lower than that of lift at speeds above 10 m/s. This study offers an innovative approach to sustainable aircraft design and energy efficiency.

Keywords: Solar energy, aircraft design, aerodynamics, NACA airfoil, flight performance.

Model Uçaklarda Güneş Panellerinin Entegrasyonu: Enerji Verimliliği ve Aerodinamik Performansın Değerlendirilmesi

ÖZ

Bu çalışma, kanatlarında güneş paneli hücreleri bulunan bir uçağın tasarım ve pratik uygulamasını içeren bir durum çalışmasıdır. Uçuş sırasında gerekli enerjinin bir kısmının yenilenebilir bir enerji kaynağı olan güneşten sağlanması hedeflenmektedir. Araştırma, güneş hücrelerinin yenilikçi bir uçak tasarımındaki etkinliğini ve uçağın çeşitli hız koşullarındaki uçuş performansını değerlendirmektedir. Prototip uçak, 2,5 m kanat açıklığı, 1,4 m uzunluk ve 0,5 m genişlikte, NACA 2412 kanat profili ile tasarlanmıştır. Farklı uçuş hızlarında (1, 5, 10, 13 ve 20 m/s) yapılan aerodinamik testler, aerodinamik kuvvetler, tork değerleri ve güneş panellerinin enerji katkısını belirlemiştir. Sonuçlar, güneş panellerinin uçuş için gerekli enerjinin %15'ini sağladığını ve 20 m/s hızda maksimum kaldırma kuvvetinin 10,68 N olduğunu göstermektedir. Uçuş hızının artması, sürükleme ve kaldırma kuvvetlerini artırmakta, 10 m/s üzerindeki hızlarda sürükleme kuvvetindeki artış oranı, kaldırma kuvvetine göre %25 daha düşük olmaktadır. Çalışma, sürdürülebilir uçak tasarımı ve enerji verimliliği konularında yenilikçi bir yaklaşım sunmaktadır.

Anahtar Kelimeler: Güneş enerjisi, model uçak tasarımı, aerodinamik, NACA kanat profili, uçuş performansı.

1. INTRODUCTION

The first solar-powered unmanned aerial vehicle (UAV), Sunrise I, was developed in 1974, and in 1975, Sunrise II was produced with aerodynamic improvements and increased power capacity. In 1980, the first successful solar-powered flight was conducted with Gossamer Penguin [1]. Subsequently, NASA launched the Pathfinder, Pathfinder Plus, Centurion, and Helios projects for purposes such as atmospheric measurements, surveillance, and communication relay. These projects offered advantages such as lower costs and flexible orbit control compared to traditional satellites. While various parameters such as wingspan, aspect ratio (AR), payload capacity, and weight estimation methods were examined for the solar-powered UAV Sky Sailor, Sun Surfer was developed to enhance durability [2]. Additionally, the high-altitude, long-endurance UAV Zephyr was designed with a lightweight carbon fiber structure, silicon-based solar panels, and lithium-sulfur batteries. To reduce energy consumption, it effectively utilized thermal air currents [3]. In parallel with these pioneering works, recent studies have focused on optimizing aerodynamic performance, flight endurance, and solar energy utilization in both fixed-wing and hybrid UAV platforms. Wang and Zhou highlighted the stability limitations of a solar-powered flying-wing UAV under low-speed conditions, recommending design improvements to enhance performance [4]. Noth et al. demonstrated that continuous flight during daylight hours is achievable through proper aerodynamic shaping

*Sorumlu Yazar (Corresponding Author)
e-posta: cuneyd.demir@ahievran.edu.tr

and energy management [5]. Barcons Ventura investigated the aerodynamic implications of solar panel integration on commercial aircraft wings, suggesting that careful panel placement can mitigate adverse aerodynamic effects while yielding additional energy gains [6]. Dinca et al. emphasized the trade-off between increased solar energy harvesting and the associated aerodynamic penalties when enlarging the panel surface area [7]. Similarly, Liscouët-Hanke et al. found that solar panel integration into seaplanes could significantly improve energy efficiency without inducing severe aerodynamic penalties if designed properly [8]. Chu et al. experimentally validated that solar panel integration can effectively extend flight endurance in small-scale UAVs [9]. The AtlantikSolar project further demonstrated the feasibility of long-duration operations by achieving an 81-hour continuous flight record with a solar-powered UAV [10]. Jaszczur et al. investigated the aerodynamic effects of panel integration on NACA airfoils, concluding that while the impact is negligible at low angles of attack, it can cause notable lift reductions at higher angles [11]. Peciak et al. examined VTOL fixed-wing UAVs, reporting acceptable structural and aerodynamic performance despite the additional mass of solar panels [12]. Liller et al. successfully demonstrated daytime autonomous flight capability using a battery-free UAV powered solely by solar energy [13]. Gao et al. introduced an energy management strategy optimized for solar-powered UAVs, reducing energy consumption during climb and glide phases [14]. Finally, El-Atab et al. provided a comprehensive review of solar-powered UAV technologies, identifying key challenges and offering design recommendations for future systems [15].

NACA series airfoil profiles are frequently preferred in aerospace engineering due to their distinctive shapes and predictable aerodynamic characteristics [16]. Aerodynamics is a critical component that directly impacts vehicle performance across a broad spectrum, from wind turbines to unmanned aerial vehicles and commercial aircraft [17]. In this context, airfoil profiles are the cornerstone of aerodynamic design; the curvature and shape of the profile are meticulously designed to generate lift and efficiently manage airflow. Specifically, the NACA 2412 airfoil profile has demonstrated its significance in this field through extensive research and studies [18]. The aerodynamic properties of the airfoil directly influence flight performance, lift generation, and energy efficiency [19]. Proper shaping and sizing optimize airflow, reduce drag, and enhance stability. Therefore, an effective airfoil design is crucial for achieving successful aircraft performance. One widely adopted method for predicting the aerodynamic performance of horizontal axis wind turbines is the Blade Element Momentum (BEM) theory [20]. This approach is favored for its relatively low computational requirements. However, the accuracy of load predictions using BEM is contingent upon the reliability of airfoil characteristic data. As the turbine blades rotate, the centrifugal force influences the boundary layer flow toward the blade tip, while the Coriolis force generates a favorable pressure gradient that directs airflow toward the trailing edge [21]. These dynamics lead to a thinner boundary layer and a shift in the flow separation point toward the trailing edge, resulting in an increase in the stall angle of attack during rotation compared to static conditions — a phenomenon known as stall delay. Because of these differing aerodynamic characteristics between rotating and static conditions, two-dimensional airfoil data requires aerodynamic corrections for accurate BEM performance predictions [22]. Various models, developed through theoretical analysis and experimentation by researchers such as Snel et al., Du and Selig, and Chaviaropoulos and Hansen, provide frameworks for these corrections [23-24]. BEM is useful for simulating the overall performance of blades by integrating general airfoil data and flow characteristics, and this has been considered in the simulations.

The efficiency of these applications relies heavily on the aerodynamic shape, and the understanding of their behavior under different conditions. A fundamental aspect of this is the prediction of lift (L) and drag (D) forces, which are essential for achieving optimal performance. Lift and drag are aerodynamic forces resulting from an aircraft's movement through the air. While lift counters the weight opposing the pull of gravity, thrust generated by propellers must overcome drag caused by air resistance. For an aircraft to take off, the thrust must exceed drag, and lift must surpass weight. In steady, level flight at constant speed, thrust balances drag, and lift equals weight [25-26]. The NACA 2412 airfoil profile was analyzed in a study examining 2D and 3D external flow at low and high speeds using ANSYS Fluent simulations and experimental data [27]. It was observed that the lift and drag forces of the NACA 2412 airfoil increased up to an angle of attack of 38°, but the lift-to-drag ratio began to decrease after 6°. Additionally, analyses conducted at a speed of 4.3 m/s indicated that the stall angle for this airfoil is 38° [28]. Moreover, under NATO AVT-252, uncertainty quantification (UQ) methods used for evaluating uncertainties on the NACA 2412 profile were compared in terms of accuracy and efficiency [29]. Furthermore, stall tests conducted on a lightweight biplane with a NACA 2412 profile determined the stall speed to be 43 knots. ANSYS Fluent CFD simulations corroborated the formation of the stall vortex and recirculation region, showing strong agreement with experimental results [30]. These findings provide a comprehensive framework for a deeper understanding of the aerodynamic characteristics of the NACA 2412 airfoil and for optimizing its performance. With advancements in computational techniques, Computational Fluid Dynamics (CFD) has emerged as a powerful tool for simulating the aerodynamic performance of airfoils and wind turbines [31]. Despite its higher computational cost and time requirements, CFD is invaluable for providing detailed insights into flow structures, assessing flow separation regions, and validating empirical models. Additionally, airfoil

characteristics can be derived from CFD simulations of rotor dynamics, enhancing our understanding of aerodynamic behaviors [32]. As computing hardware and parallel algorithms improve, both researchers and industry professionals increasingly rely on CFD to simulate the aerodynamic performance of airfoils across various angles of attack. These simulations are crucial for developing lighter and more efficient designs, which not only improve speed but also reduce fuel consumption through the selection of lighter materials and thinner structures [33].

Optimization studies based on artificial intelligence and heuristic algorithms, developed to enhance the aerodynamic efficiency and autonomous flight capabilities of state-of-the-art fixed wing unmanned aerial vehicles, have gained significant importance. A morphologically adaptable UAV was optimized using an AI-based method to simultaneously improve directional stability and the maximum lift-to-drag ratio; the optimal sweep angle was determined using an artificial neural network and bee colony optimization [34]. The vertical tail and Autonomous Flight Control System (AFCS) of a piston-prop tactical UAV were optimized using the Simultaneous Perturbation Stochastic Approximation (SPSA) algorithm, resulting in a 49% improvement in flight performance [35]. Similarly, by simultaneously optimizing the wing sweep angle and flight control system parameters with the SPSA algorithm, autonomous flight performance was enhanced by 42%. The new design enabled faster and more stable flight even under turbulent conditions [36]. For a tactical UAV with passive and active morphable wing-tail structures, longitudinal and lateral control systems were optimized using the SPSA algorithm, achieving a 46% performance increase and enhancing flight dynamics criteria and tracking success under turbulence [37]. Moreover, to simultaneously improve roll stability and lift-to-drag ratio, a morphable UAV was redesigned using an artificial neural network and bee colony optimization. This AI-based method provided an efficient optimization process in terms of both time and cost [38]. The flight performance of a hexarotor UAV with variable arm lengths was enhanced by optimizing it with a deep neural network and the SPSA algorithm. PID coefficients and moments of inertia were simultaneously determined, resulting in effective and rapid control [39]. Additionally, the Percentile-Based Adaptive Immune Plasma Algorithm (pIPA), inspired by convalescent plasma therapy, has been successfully applied to engineering optimization problems. Thanks to its dynamic percentile approach, it has yielded superior results in both noise reduction and UAV route planning [40]. Finally, the thrust coefficient of an 11-inch quadrotor UAV propeller was examined through CFD analyses using the k-ω SST turbulence model. It was observed that as airspeed increased, the thrust coefficient decreased, and at lower speeds, numerical data aligned more closely with experimental results [41].

Various studies have employed numerical methods to analyze airfoil profiles. Analyses of the NACA0009 and NACA4415 profiles showed that the NACA4415 achieved the highest performance, with the angle of attack increase leading to higher lift and drag coefficients [42]. Research on the Eppler 423 and NACA 6409 profiles indicated that the Eppler 423 exhibited superior lift performance under low-speed conditions, while the NACA 6409 delivered better glide performance [43]. Additionally, a multi-objective optimization study on a wing chord section achieved a 5% reduction in structural mass and a 14% increase in the first natural frequency [44].

This study addresses a significant gap in existing literature, by focusing on the aerodynamic analysis of a newly designed aircraft that incorporates NACA 2412 airfoils equipped with solar panels to partially harness solar energy for propulsion. In addition to the lift and drag analyses, this research evaluates the torque values acting on the aircraft at different flight speeds. The design was tested in flight, and discussions include the normal forces, drag forces, and torque values achieved within the specified speed ranges. Moreover, contour plots for pressure, velocity, and streamlines were generated to illustrate the aerodynamic behavior of the aircraft. An RC model aircraft that generates its own power using solar energy and lithium polymer batteries was designed and manufactured as part of this study. The electrical energy produced by photovoltaic cells was regulated to optimal current and voltage levels via an electronic circuit known as a maximum power point tracker (MPPT). The generated energy was used to power the propulsion system and was stored in batteries for night flights. The results showcase flight analyses involving renewable energy power generation, contributing to the understanding of how solar energy integration can enhance overall aircraft efficiency while maintaining optimal aerodynamic performance. The findings will not only provide valuable insights for the design and development of solar-powered UAVs but also offer practical implications for future innovations in aircraft technology, paving the way for more sustainable aviation solutions. Thus, this work serves as a beneficial resource for engineers and researchers alike, fostering advancements in the field of aerodynamics and renewable energy applications in aviation.

2. THEORETICAL FRAMEWORKS

Studies on utilizing solar energy have gained significant importance. Solar energy systems have advanced technologically, become more affordable, and are now widely accepted as an environmentally friendly energy source. Due to its advantages, the use of solar energy in aircraft is increasingly popular.

An RC or autonomous model aircraft has been designed for applications such as land surveying, imaging, mapping, and damage assessment after natural disasters. This model aircraft is equipped with a solar-powered

system that stores energy, allowing for long-distance flights without harming the environment. It is developed to perform its flight along the given coordinates with an eco-friendly approach. The aircraft can autonomously complete its flight along designated coordinates, and it can be controlled remotely via radio control.

The NACA 2412 airfoil is an ideal choice for training aircraft, light sport aircraft, and certain unmanned aerial vehicles due to its high lift capability and low drag coefficient at low speeds. With moderate camber and a 12% thickness, it provides aerodynamic stability, making it a safe and easy-to-handle option for novice pilots in training. Economically advantageous, this airfoil reduces operating costs by offering fuel efficiency, which is particularly beneficial for training and recreational aircraft. Its versatility also makes it suitable for both commercial and private use. The 12% thickness ratio enhances structural durability, offering a long-lasting and robust option for light aircraft and UAVs. Thanks to these characteristics, the NACA 2412 holds a significant place in general aviation and UAV applications as an economical, reliable, and versatile airfoil. In light of this information, the NACA 2412 airfoil has been used on the model aircraft.

2.1 Geometry

In this study, a model aircraft was designed with the aim of conducting reconnaissance and observation flights at low speeds. The fabrication and assembly processes were completed, followed by flight testing. The design commenced with the selection of one of the most critical components of the aircraft – the airfoil. The reason for selecting the NACA 2412 airfoil for solar cell placement is its asymmetric structure, which provides a high lift coefficient, enhancing efficiency in energy production. This airfoil offers a broad upper surface area, allowing solar cells to be positioned more effectively. Additionally, the low drag coefficient of the NACA 2412 minimizes energy consumption during flight. The angled upper surface can capture sunlight from a wider range of angles, increasing its energy collection capacity.

The NACA 2412 airfoil's asymmetric design differs from symmetric profiles (e.g., NACA 0015 or NACA 0021). Asymmetric profiles generate higher lift than symmetric ones. This is advantageous, especially when carrying solar cells. While symmetric profiles provide the same aerodynamic properties on both surfaces, asymmetric profiles, like the NACA 2412, offer a larger area and greater inclination on the upper surface, enabling a more efficient placement of solar cells. Furthermore, the ability of the NACA 2412 to produce high lift at lower angles of attack supports energy efficiency during flight, a feature typically unattainable with symmetric profiles.

The model aircraft is a single-propeller design powered by a DC brushless motor. It has a length of 140 cm, a height of 50 cm, a wingspan of 250 cm, a wing width of 30 cm, and a total weight of 2.6 kg, including all internal components. The aerodynamic body structure was considered in the design of the mechanical assembly (Figure 1). The selection of a DC brushless motor is based on thrust values. Once the motor is chosen, other electronic components are determined accordingly. The amount of thrust required for the model aircraft's take-off and flight should be between 1.3 and 1.8 times the aircraft's weight. The minimum thrust value has been calculated as 3380 g based on 1.3 times the weight, and the maximum thrust value as 4680 g based on 1.8 times the weight. Considering all calculations and component selections, the combination of the Emax GT3526/05 (710KV) motor [45], a 5S 5000mAh 30C LiPo battery, a 13x7 inch propeller, and the Skywalker 60A ESC offers a suitable system for an RC aircraft weighing 2.6 kg, ensuring sufficient lift and thrust production. The wing surface area (0.75 m²) and lift force support flight stability and takeoff. With the 5S LiPo battery (18.5V) and 13x7 inch propeller, this setup can generate 3500 g of thrust. The aircraft's minimum thrust requirement is 3380 g, and the maximum thrust requirement is 4680 g. The available thrust capacity meets the minimum requirement, ensuring the system design is optimized to deliver sufficient performance for flight (Table 1).

Table 1. Model aircraft components

Component	Selection
Brushless DC Motor	Emax GT3526/05 (710KV)
Propeller	13x7 inch
Battery	5S 5000mAh 30C LiPo
ESC	Skywalker 60A ESC
Autopilot	Ardupilot APM
Servo Motors	8g x 5
Solar Panels	54 x Solar Cell (1 Watt) Monocrystalline PV, STC 2A, 0.5 V
DC/DC Converter	MPPT (75 Watt)

The project incorporates a brushless electric motor, ESC (Electronic Speed Control), APM (Ardupilot Mega), Li-Po (Lithium-Polymer) battery, servo motors, remote control, telemetry, solar cell, and MPPT components. The model aircraft utilizes a photoboard (compressed foam) material, which is both lightweight and more durable than other foam materials. The system includes a total of five servo motors: two on the wings, two on the tail, and one on the front wheel. The ESC output connected to the motor and the five servo motor outputs are linked to the APM unit. This setup, with pre-programmed software on the APM unit, ensures safe takeoff, flight, and landing along specified coordinates. Test flights have been conducted with manufactured model aircraft, yielding positive results each time.

The operational structure of the model aircraft is as follows: the DC motor is controlled by an ESC (Electronic Speed Control), which regulates the voltage supplied to the motor, thereby controlling its rotation speed. The reference position and required coordinates are provided to the ESC by the APM (autopilot) board, enabling the model aircraft to perform its movements. To supply energy, a total of 54 solar cells are mounted on the wings. These cells are divided into two sets of 27, with

each set connected in series. Each solar cell generates 0.5 V, resulting in a total voltage of 27 V. This 27 V output is directed to a DC/DC converter known as a maximum power point tracker (MPPT), which tracks the peak power generated at specific intervals and directs it to the load, supplementing the energy of the Li-Po battery.

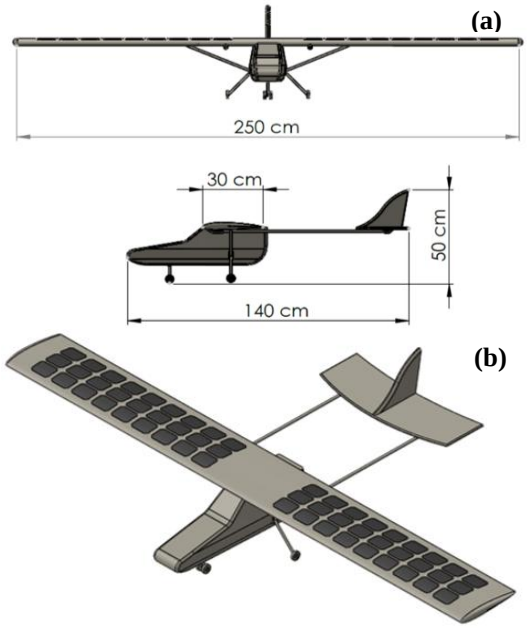

Figure 1. (a) Length, height, and wingspan (b) Aircraft design

For protection, a transparent epoxy resin coating was applied over the solar cells and the conductive wires connecting them to prevent any damage. The model aircraft's safe flight duration was initially determined to be 2 minutes, which was extended to 2 minutes and 20 seconds with the addition of solar energy (Figure 2).

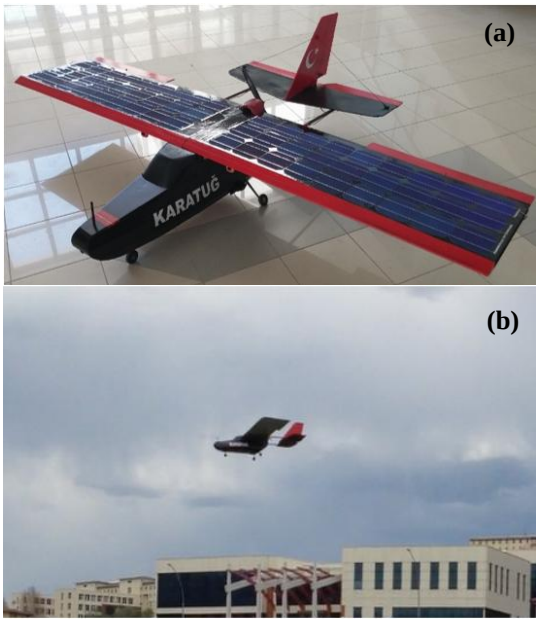

Figure 2. (a) Manufactured model aircraft (b) Model aircraft test flight

3. METHODOLOGY

A substantial portion of the data presented in this study was obtained from computational fluid dynamics (CFD) simulations conducted using specialized software. In addition, short-duration real flight tests were carried out with the fabricated model aircraft, and relevant observations were made.

3.1. Estimation of Annual Energy Output from Photovoltaic Solar Installations

Aircraft motor power is typica

lly supplied by fixed-capacity batteries. The flight duration is directly related to the battery capacity. For the produced model aircraft, the incorporation of solar cells on the wing surfaces aims to extend flight duration or optimize battery usage. The calculation of power that can be obtained from the panels is provided in Equation 1. The daily energy output of a photovoltaic (PV) solar installation can be estimated using this equation [46]:

$$P = A \times r \times H \times PR \quad (1)$$

The power output (P) of a solar panel system is determined using several key factors. These include the total area of the solar panels (A) measured in square meters (m²), the yield or efficiency of the solar panels (r), which is expressed as a percentage, and the annual average solar radiation incident on tilted panels (H), given in kilowatt-hours per square meter per day (kWh/m²/day), excluding shading effects. Additionally, the performance ratio (PR), a dimensionless coefficient accounting for various losses in the system, also plays a crucial role. The performance ratio typically ranges between 0.5 and 0.9, with a default value of 0.75 often used for calculations. Together, these parameters provide a comprehensive understanding of the solar panel system's potential power output.

The general linearization equation for nonlinear dynamics is expressed as $\dot{x} = F(x, u)$ where x represents position and u represents velocity [47]. Taherinezhad et al. [48] developed nonlinear equations as a function of time steps. This approach can be directly applied to the model for evaluating the flight angle for further investigation.

3.2. Program Set Up and Mesh Independence Test

Establishing the fundamental requirements for solution analysis, the initial and boundary conditions have been defined for the system. Standard conditions for air at 1 atm pressure and 25°C were specified for the flow domain. The solar radiation amount is defined in the program as a regional average of 600 W/m². This value is also considered a global average for harnessing solar radiation effectively. To create five distinct boundary conditions, five different velocity values in the x-direction (1, 5, 10, 13, and 20 m/s) were designated as inlet velocity boundary conditions for the flow region. The k-ε turbulence model was employed for the analysis,

as it was deemed sufficient to provide the flow lines in the simulation results. It is possible to continue the analyses for all variables and varying environmental conditions [31-33].

All regions where the airflow interacts with the aircraft are characterized as solid-fluid interfaces, which is critical for determining flight effects. The remaining surfaces of the flow domain were treated as open pressure boundary conditions, which exhibit no direct influence on the airflow region. In the external flow option, cavitation regions devoid of flow were excluded. The effects of gravity were taken into account. For the solution analysis, forces and torque values were targeted, as they were deemed to have a direct impact on flight. Since the variation of the angle of attack was also of interest, the aerodynamic angle option was not utilized. Accurately determining the forces in the x, y, and z directions is crucial for assessing the angle of attack. The drag force (x) and lift force (y) values obtained within the established Cartesian coordinate system were evaluated for their impact on the aircraft's flight performance. All target solutions were completed to an accuracy of 10^{-2}. The distribution of the mesh and cells over the airfoil is presented in Figure 3a.

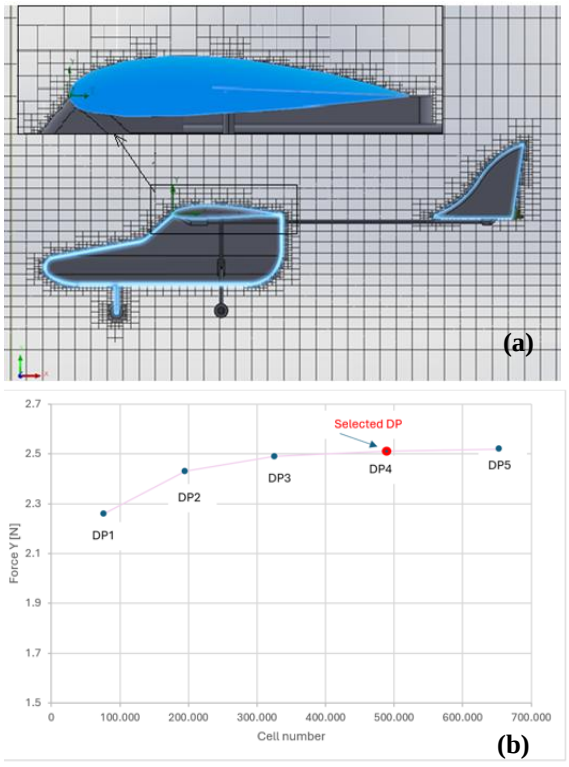

Figure 3. (a) Mesh structure (b) Mesh independency

Creating a quality mesh structure for aerodynamic problems is paramount. When determining the fundamental mesh for outflow challenges of this nature, a denser cell structure was employed in regions close to the airfoil. The global mesh was set to a fourth-order quality with a ratio factor of 5.5, emphasizing the need for small cells enhancing resolution in areas affecting the flow. An equidistant refinement mesh of third order (offset distances of 0.1 and 0.5 mm) was applied in sections near the solid-fluid interfaces to ensure reliable calculations. To ascertain the independence of the solution from the mesh structure and cell count, comparisons were made using design points with 5 different cell counts (76,871; 195,324; 325,639; 489,291; and 652,754), with a specific focus on the drag force results. The solution obtained with a total of 925,208 cells at the fourth design point, including 489,291 cells in contact with solid regions, was deemed sufficient. Since increasing cell counts did not significantly affect the solution outcomes, all subsequent analyses were concluded under the conditions of design point 4, thereby saving computational time. The relationship between cell counts and drag force variations is illustrated in Figure 3b.

4. RESULTS AND DISCUSSIONS

While the integration of solar panels enhances the aircraft's energy autonomy, it introduces certain trade-offs. The additional weight of approximately 450 grams due to the solar panels, protective epoxy coating, and MPPT system increases the overall mass by nearly 17%. This increase affects the lift-to-weight ratio and slightly raises the minimum required thrust. Additionally, the cost of integrating high-efficiency photovoltaic cells and associated electronics contributes to the overall project budget. However, the 15% contribution to flight energy and the 16.6% extension in flight duration (from 120 s to 140 s) observed during test flights demonstrate that the benefits of solar integration compensate for the added weight and cost. Especially for UAV applications, where extended loitering times are crucial, such trade-offs are deemed acceptable considering the operational advantages gained.

The observed 16.6% improvement in flight duration, although seemingly modest, carries significant practical implications, particularly for UAV missions such as mapping, surveillance, or environmental monitoring. In autonomous missions where every additional minute of endurance extends the coverage area or operational capacity, this improvement directly translates into increased efficiency and mission success rates. For example, in search and rescue operations or post-disaster assessments, even slight increments in flight time can provide critical additional data. Moreover, the reduction in battery consumption due to solar contribution can prolong battery life and reduce maintenance costs, further supporting the operational benefits of solar integration.

In the present study, the flow was assumed to be steady, incompressible, and laminar, which is a valid approximation due to the low Reynolds number associated with the flight speeds of the model aircraft. The computational domain was subjected to five inlet boundary conditions corresponding to freestream velocities of 1, 5, 10, 13, and 20 m/s, uniformly applied

at the inlet section to simulate different flight regimes. The aircraft surfaces, including the wing, fuselage, and solar panels, were modeled as no-slip walls, enforcing zero velocity at the solid boundaries to accurately capture boundary layer effects. The outlet boundary was defined as a pressure outlet with a fixed atmospheric pressure condition to allow for smooth flow exit without artificial reflections. The far-field boundaries of the domain were also treated as pressure outlets to emulate the undisturbed external flow conditions. Gravitational acceleration was incorporated into the simulations to account for its effect on aerodynamic forces and torque. Standard atmospheric properties of air were considered, with a density of 1.225 kg/m³ and a dynamic viscosity of 1.7894×10^{-5} Pa·s, at an ambient temperature of 25°C and a reference pressure of 1 atm.

4.1. Flow Contours on Front Plane on The Origin

The velocity and pressure contours of the aircraft at a planar flight speed of 10 m/s for a central flow layer are presented in Figures 4a and 4b, respectively.

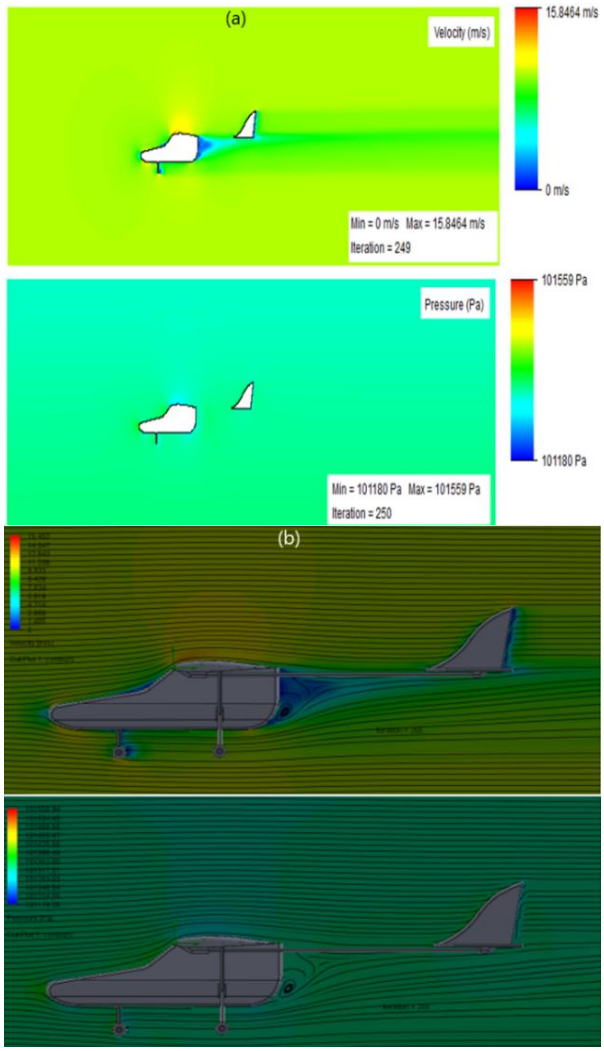

Figure 4. (a) Flow contours (b) Flow streamlines

Notably, high velocity gradients were observed over the airfoil. Regions of low pressure and turbulence, an expected phenomenon, developed behind the airfoil and at the rear of the aircraft fuselage. This indicates that the results obtained around the airfoil suggest a particularly advantageous geometry for the flow. The fuselage, being appropriately aligned with the airfoil, did not generate any significant velocity or pressure gradients that would adversely affect the flow. The variation of velocity and pressure showed similar trends across all specified speed values. Determining streamlines alongside the formation of pressure and velocity gradients during the motion of the aircraft is also beneficial for understanding the overall flow behavior. As illustrated in Figure 4-b, streamlines provide valuable insights into the trajectory of airflow around the aircraft, highlighting how the airflow interacts with the surfaces of the wings and fuselage. The significance of streamlines lies in their ability to visualize the direction of fluid flow, which helps in identifying regions of potential lift generation and drag. Moreover, analyzing the forces acting on the aircraft, such as lift, drag, and induced effects, is essential for optimizing aerodynamic performance. By studying these streamlines, one can discern how the shape and orientation of the aircraft influence the surrounding airflow, ultimately informing design choices and improving flight efficiency.

4.2. Streamlines on The Aircraft

The variations in Mach number at the interfaces between the aircraft and the flow region are presented in Figure 5. As shown in the figure, the formation of low-flow regions behind the wings directly affects flight, and this occurrence is consistent with the flight simulations conducted by Khan et al. [50]. These changes in Mach numbers are critical as they indicate the speed of the airflow relative to the speed of sound in the local medium. In areas where the Mach number approaches or exceeds 1, compressibility effects become significant, which can lead to changes in the aerodynamic characteristics of the aircraft. For instance, regions of supersonic flow can result in shock waves, which can dramatically impact lift and drag forces, influencing the overall performance and stability of the aircraft. Additionally, the distribution of Mach numbers around the aircraft surfaces provides insight into the flow regime, allowing for the identification of areas that may experience increased aerodynamic pressure loads or potential flow separation. Understanding these Mach number distributions is essential for predicting the aircraft's behavior in various flight conditions and ensuring optimal aerodynamic design.

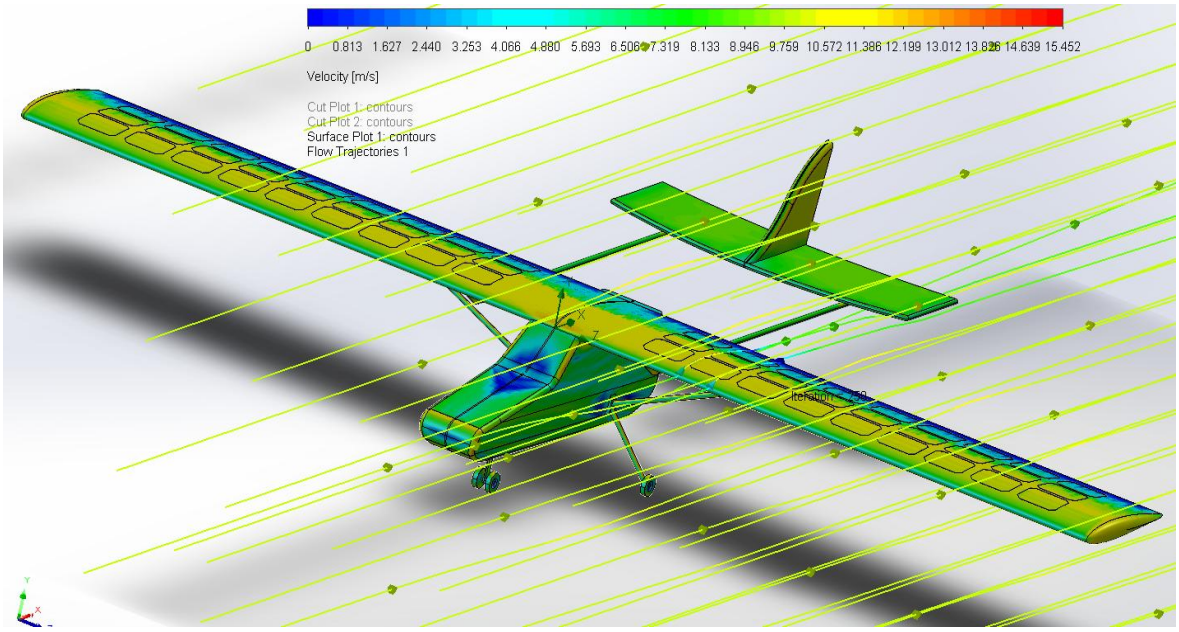

Figure 5. Flow trajectories on the aircraft

4.3. Solar Panel Power Evaluation

A 1200 W capacity battery was selected based on the engine power that was chosen for the designed and produced aircraft. To enhance flight duration and enable economic operation, solar panels have been integrated with systems capable of directly supplying the battery systems. The average daily solar radiation values were selected from the NASA Power database for the conditions in Kırşehir (Latitude: 39.13, Longitude: 34.20) [49]. An assessment of the potential power generation was performed for the range of solar radiation values, based on the specifications of the panels.

Figure 6 illustrates the power output provided by the solar panel and its contribution to the 1200 W battery power under varying solar irradiation conditions (see eq. 10). Here, losses due to the inverter and temperature are accounted for as 8%, cable losses as 2%, and other losses (such as shading) as 3%. Considering a total panel area of 0.55 m² and an efficiency rating of 15%, the solar power output ranges from 46 W under the lowest solar radiation conditions to 186 W under the highest. Considering the total battery capacity, the solar cells can generate an additional power output ranging from 3.83% to 15.5%. In the absence of other contributing factors, this percentage should be acknowledged, as having a direct impact on increasing flight duration. The flight duration of the model aircraft, performed at maximum speed (20 m/s), was extended from 120 seconds to 140 seconds with the support of solar cells. This approximately 16.6% increase in flight duration was found to be consistent with theoretical calculations. It is clear that the relatively low efficiency of the solar panel and the solar radiation values in the chosen region could be improved, thereby enhancing energy generation. It is recommended that this prototype be further developed.

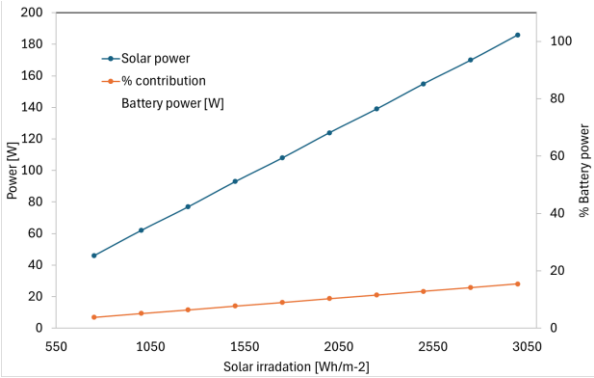

Figure 6. Power change according to solar radiation

4.4. Forces Affecting Flight and Torque Evaluation

The effects of variations in aircraft speed on drag (Force X) and lift (Force Y) are illustrated in Figure 7. As expected, an increase in speed leads to an increase in both of these aerodynamic forces. In the context of validation, the 3D computational analysis of UAV drones conducted by Khan et al. [50] determined the forces acting on the aircraft at a speed of 35 m/s based on the angle of attack. At a zero angle of attack, corresponding to level flight, the Y-normal force was measured at 50 N. The observed increasing trend in the Y force illustrated in the figure supports the possibility of yielding forces that are close to this determined value.

In the conducted simulation, the takeoff and landing conditions were not directly studied. This is because additional factors, such as the geometric position of the aircraft, come into play. Instead, the aim was to identify the forces acting on the aircraft during free flight at low speeds. Simulating the effects of weight during takeoff and landing would be beneficial for future studies.

The flight speed values provided, ranging from 1 to 20 m/s, are measurements taken for the model aircraft being tested. Considerations for flights at higher speeds were not included, as they exceed the specified motor power, which necessitates the use of a stronger motor. Although the increase in drag and lift forces below 10 m/s, shows a similar trend, the growth in lift force values above this speed is relatively more pronounced. This suggests a positive contribution to the aircraft's ability to ascend. Furthermore, the effects of acceleration can be interpreted as directly proportional to the power provided by the motor. This relationship highlights the importance of thrust in enhancing both lift and overall aircraft performance during flight. During level flight, the force in the Y direction is greater than the force in the X direction and this ratio increases with the acceleration of speed suggesting a reduction in both gravitational and angular effects. Furthermore, at the specified flight speeds, it can be inferred that the Y force, when managed by appropriate control systems, can enhance the aircraft's capability for altitude gain. It should be noted that the weight of the aircraft and, consequently, the effects of gravitational forces will have a direct impact on this context. Conversely, the X forces indicate that the ability to yaw (rotate about the vertical axis) is inversely proportional to the speed, thereby indicating limitations (by about 60% compared to the altitude gain) in the aircraft's maneuverability.

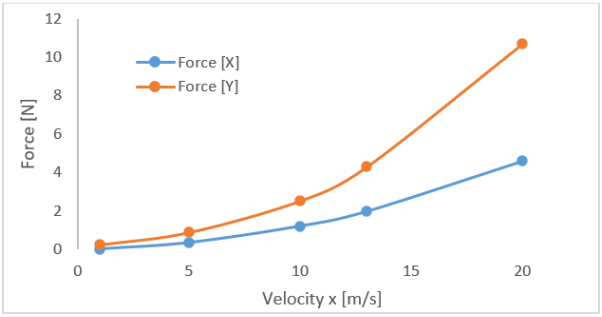

Figure 7. Drag and lift forces

Similarly, the values of global drag forces are directly related to flight speed, as shown in Figure 8. The relationship between drag and speed consists of two components: parasite drag, which is proportional to the square of velocity, and induced drag, which is inversely proportional to the square of velocity. The drag values in other directions are generally higher compared to the drag experienced during forward flight, as aircraft are designed to minimize drag in that orientation. This is to be expected in well-designed fuselage and wing configurations, where the aerodynamic characteristics are optimized for smooth airflow. Such a relationship has been established across all speed conditions, demonstrating the importance of minimizing drag to enhance flight performance and efficiency. By reducing drag, the aircraft can achieve better speed retention and maneuverability, ultimately contributing to improved operational effectiveness. In summary, the frictional effects in the vertical direction are negligible, indicating that the aircraft has an appropriate geometric design. On the other hand, the horizontal drag force experienced during level flight is directly related to the flight speed, and flights at speeds exceeding 20 m/s are not recommended for the specified design.

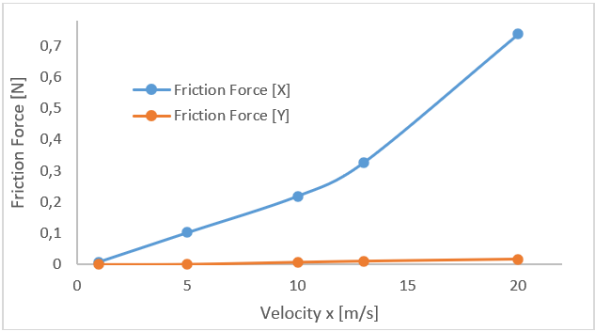

Figure 8. Friction forces for global coordinate

It is also beneficial to determine the drag forces on the surfaces of the selected airfoil type (NACA 2412). Figure 9 illustrates the effect of varying speeds on these forces. It is evident that the forces experienced on the airfoil surface are considerably lower compared to the global drag forces. Such results are expected for this standardized design, which is widely accepted under typical flight conditions. The findings validate analytical conditions, confirming that the chosen airfoil exhibits favorable aerodynamic properties. This lower drag on the airfoil surface contributes to enhanced flight efficiency and performance, supporting the effectiveness of the NACA 2412 design in various operational scenarios. For the prototype designed in this study, the shear drag in the Y-direction is negligible. Conversely, the shear drag in the X-direction exhibits a tendency to increase at an acceptable level within the specified speed range.

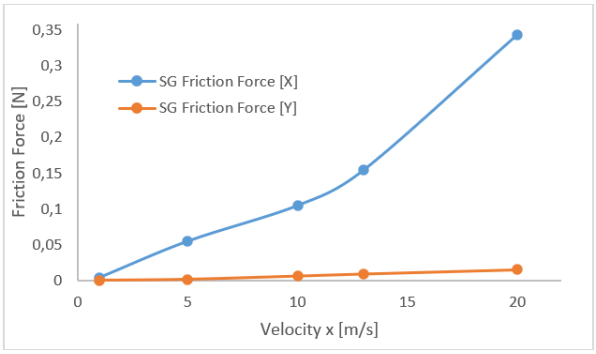

Figure 9. Friction forces for the airfoil surface

In our simulation study of airflow effects during aircraft flight, we specifically analyzed the drag and lift forces, alongside global and surface friction forces. We examined how these values varied within the specified flight speed range and discussed the implications of these

changes. Additionally, we determined the torque values and their variations at different speeds. The analysis revealed that torque plays a significant role in the overall aerodynamic performance of the aircraft. Variations in torque can influence the aircraft's stability and control, particularly during maneuvers such as climbs, turns, and descents. Higher torque values at increased speeds may contribute to a greater rotational force, enhancing the aircraft's responsiveness and agility. Conversely, at lower speeds, reduced torque can lead to a less responsive handling experience. Understanding the interplay between torque and flight dynamics is crucial for optimizing aircraft design and ensuring safe and efficient operations, particularly in varying flight conditions. This variation is illustrated in Figure 10. It was determined that the increase in speed significantly affects the global torque values that are valid for all computational domains in the y-direction, demonstrating an inversely proportional relationship. As flight speed increases, the corresponding torque in the y-direction changes to highlight the dynamics of the aircraft's stability and control. This relationship is critical, as it indicates that higher speeds could lead to decreased stability in the y-direction, necessitating careful management of control inputs by the pilot. Understanding these torque changes is essential for predicting the aircraft's behavior during various flight profiles, aiding in the design of more stable and controllable aircraft configurations. Adapting control systems to account for these changes can enhance overall flight safety and performance.

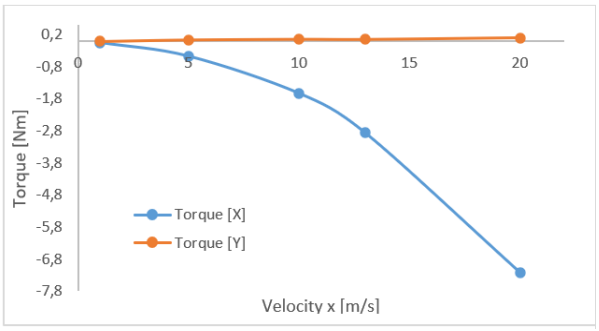

Figure 10. Global tork

Based on our analysis, it can be concluded that the generated torque values are adequate for ensuring safe flight conditions. Furthermore, the presence of negative torque in the Y-direction is contributing sufficiently to the aircraft's ability to ascend by changing the flight angle. This suggests that the designed torque characteristics are favorable for enhancing the aircraft's lift during flight, thereby supporting the overall stability and performance of the aircraft in various flight profiles.

5. CONCLUSION

This study has provided valuable insights into the aerodynamic performance of a novel aircraft utilizing the NACA 2412 airfoil, incorporating solar energy panels to enhance flight duration. By examining the interplay between airflow dynamics, drag and lift forces, and torque variations at various flight speeds, we have established a comprehensive understanding of the aircraft's operational characteristics. The effective method employed for calculating the airfoil's surface positions using cosine spacing, in conjunction with a rigorous mesh independence test, has ensured accuracy and reliability in aerodynamic analysis. The advantageous velocity and pressure contours around the fuselage indicated optimal airfoil-fuselage configuration, demonstrating minimal turbulence and pressure gradients. Additionally, the analysis revealed significant trends in airflow characteristics, particularly related to the Mach number, which is critical for understanding potential supersonic flow and its impact on drag and lift. The proportional relationship between flight speed and aerodynamic forces was reinforced; with increased speeds leading to enhanced drag and lift, including a maximum lift of 10.68 N at 20 m/s. The integration of solar panels contributed 15% of the required energy, with potential power generation assessed against solar radiation conditions in Kırşehir, Türkiye. Moreover, during level flight, the predominance of the Y-direction force over the X-direction force suggests an improved capacity for altitude gain, while highlighting limitations in yawing capability. The torque evaluation underscored its dynamic role in aircraft stability, with findings indicating that the designed torque characteristics support enhanced lift and stability during various maneuvers, necessitating precise control management. Overall, this study confirms that the combination of aerodynamic design and solar energy integration considerably contributes to flight efficiency and performance, setting the stage for future advancements in aircraft design and aerodynamic optimization.

This research makes a significant and novel contribution to the fields of aerodynamics and renewable energy integration for aircraft by systematically filling key gaps in the existing literature.

- Bridging simulation and experiment: While many previous studies were limited to numerical or theoretical analysis, this study integrates both CFD results and real-world flight data, establishing a validated correlation between simulations and actual aircraft behavior under solar-assisted flight conditions.
- Inclusion of torque in aerodynamic assessment: Unlike conventional works, this study systematically analyzed torque variations, providing a more holistic understanding of the aircraft's stability and control characteristics. It was determined that a torque of 7.8, Nm could be produced at the specified maximum speed of 20 m/s.
- Quantification of real-time solar energy contribution: Through MPPT-controlled solar energy management, the research quantifies the operational benefits of solar integration, verifying a 16.6% endurance enhancement through experimental flight testing.

- Minimization of aerodynamic penalties: Despite surface modifications caused by solar panel integration, the aircraft maintained a favorable aerodynamic performance due to optimized design using the NACA 2412 airfoil. The static friction force increased with speed, reaching a maximum value of 0.38 N. For the normal friction force, this value was found to be 0.69 N. At the maximum speed of 20 m/s, the drag and lift forces were calculated to be 3.2 N and 10.8 N, respectively.
- Comprehensive and unified analysis: Combining CFD-based aerodynamic evaluation, torque behavior analysis, solar energy modeling, and experimental verification within a single study provides a holistic and practically applicable framework for future UAV designs.

In conclusion, this work presents one of the most complete and experimentally validated frameworks for the aerodynamic and energetic evaluation of solar-powered aircraft. The findings not only advance academic knowledge but also provide valuable practical guidelines for the development of sustainable, efficient, and autonomous UAV systems. The combination of validated aerodynamic performance, energy efficiency, and flight stability confirms the feasibility and benefits of integrating renewable energy sources into modern UAV designs.

In future research, it would be highly valuable to examine the integration of alternative photovoltaic technologies, such as perovskite-based, CIGS, or multi-junction solar cells, which offer superior efficiency to weight ratios compared to conventional silicon-based systems. Furthermore, the development of advanced integration strategies – including conformal, embedded, or aerodynamically optimized solar panel configurations - holds the potential to mitigate adverse aerodynamic effects while maximizing energy harvesting capabilities. The incorporation of hybrid power architectures, combining solar energy with supplementary renewable sources such as fuel cells or micro wind turbines, could also be explored to enhance energy autonomy and operational endurance under diverse flight conditions. In parallel, future studies may focus on the structural optimization of aircraft specifically designed for solar energy integration, where aerodynamic performance, structural integrity, and energy efficiency are simultaneously considered. Lastly, the implementation of intelligent and adaptive energy management systems capable of dynamically optimizing the distribution of solar, battery, and propulsion power according to flight conditions may significantly improve the overall performance and endurance of solar-assisted aircraft, especially for autonomous and long-endurance applications.

Furthermore, while this study employed only a lithium-polymer (Li-Po) battery as the energy storage system, future studies may explore hybrid energy management architectures incorporating supercapacitors alongside battery units. These hybrid configurations could effectively address the transient power demands associated with solar energy input, while also offering benefits in terms of smoothing power fluctuations and extending battery lifespan.

DECLARATION OF ETHICAL STANDARDS

The author(s) of this article declare that the materials and methods used in this study do not require ethical committee permission and/or legal-special permission.

AUTHORS' CONTRIBUTIONS

Cüneyd DEMİR: Contributed to the study's conception and design, conducted data analysis, and drafted the manuscript.

Merdin DANIŞMAZ: Assisted with data collection and interpretation and critically revised the manuscript for important intellectual content.

Ahmet KÖROĞLU: Provided guidance on methodology and statistical analysis, supervised the project, and ensured the accuracy of the results.

All authors approved the final version of the manuscript and agree to be accountable for all aspects of the study.

CONFLICT OF INTEREST

There is no conflict of interest in this study.

REFERENCES

[1] Boucher R., "History of solar flight", ***20th Joint Propulsion Conference***, Cincinnati, OH, USA, June 11-13, pp. 1429, (1984).

[2] Nickol C.L., Guynn M.D., Kohout L.L. and Ozoroski T.A., "High Altitude Long Endurance Air Vehicle Analysis of Alternatives and Technology Requirements Development", ***In Proceedings of the 45th AIAA Aerospace Sciences Meeting and Exhibit***, Reno, CA, USA, 8–11 January, pp. 12653–12669, (2007).

[3] Al Dhafari L.S., Afzal A., Al Abri O.K. and Khan A., "Solar-Powered UAVs: A systematic Literature Review," ***2nd International Conference on Unmanned Vehicle Systems-Oman (UVS)***, Muscat, Oman, 12-14 February, pp. 1-8, (2024).

[4] Wang K. and Zhou Z., "An investigation on the aerodynamic performance of a hand-launched solar-powered UAV in flying wing configuration," ***Aerospace Science and Technology***, 129, 107804, (2022).

[5] Noth A, "Design of solar powered airplanes for continuous flight" (PhD Thesis), ETH Zurich, pp. 61, (2008).

[6] Barcons Ventura N, "Study of the aerodynamic and energetic impact of the solar panel's installation on a commercial plane's wing", (Master's Thesis), Universitat Politècnica de Catalunya, pp. 56, (2018).

[7] Dinca L., Corcau J. I. and Voinea D. G., "Solar UAVs-more aerodynamic efficiency or more electrical power?" ***Energies***, 16(9): 3778, (2023).

[8] Liscouët-Hanke S., Mir M. and Bashir M., "Exploration of Solar Power System Integration for Sustainable Air

Transportation-A Case Study for Seaplane Air Taxi Operations," ***Aerospace***, 12(3): 164, (2025).

[9] Chu Y., Ho C., Lee Y. and Li B., "Development of a solar-powered unmanned aerial vehicle for extended flight endurance," ***Drones***, 5(2): 44, (2021).

[10] Oettershagen P., Melzer A., Mantel T., Rudin K., Stastny T., Wawrzacz B. and Siegwart, R., "Design of small hand-launched solar-powered UAVs: From concept study to a multi-day world endurance record flight," ***Journal of Field Robotics***, 34(7): 1352-1377, (2017).

[11] Jaszczur M., Papis K., Książek M., Czerwiński G., Wojtas G., Koncewicz W. and Wójcik M., "Investigation of aerodynamic parameters of solar plane airfoil using CFD modeling," ***Computer Science***, 22: 123-142, (2021).

[12] Peciak M., Skarka W., Mateja K. and Gude M., "Impact analysis of solar cells on vertical take-off and landing (VTOL) fixed-wing UAV," ***Aerospace***, 10(3): 247, (2023).

[13] Liller J., Goel R., Aziz A., Hester J. and Nguyen P., "Development of a battery free, solar powered, and energy aware fixed wing unmanned aerial vehicle," ***Scientific Reports***, 15(1): 6141, (2025).

[14] Gao Y., Qiao Z., Pei X., Wu G. and Bai Y., "Design of energy-management strategy for solar-powered UAV," ***Sustainability***, 15(20): 14972 (2023).

[15] El-Atab N., Mishra R. B., Alshanbari R. and Hussain M. M., "Solar powered small unmanned aerial vehicles: A review," ***Energy Technology***, 9(12): 2100587, (2021).

[16] Khani Aminjan K., Ghodrat M., Heidari M., Rahmanivahid P., Naghdi Khanachah S. and Hitt M., "Numerical and experimental investigation to design a novel morphing airfoil for performance optimization", ***Propulsion and Power Research***, 12(1): 83-103, (2023).

[17] Sudin M.N., Abdullah M.A., Shamsuddin S.A., Ramli F.R. and Tahir M.M., "Review of research on vehicles aerodynamic drag reduction methods", ***International Journal of Mechanical and Mechatronics Engineering***, 14(2): 35-47, (2014).

[18] Chakraborty S. and Ghosh S., "A CFD study on the structural parameters of NACA 2412 airfoil-based air-wing using different composite materials", ***Materialstoday: Proceedings***, 60: 894-901, (2022).

[19] Danışmaz M. and Demirbilek M., "Assessment of heat transfer capabilities of some known nanofluids under turbulent flow conditions in a five-turn spiral pipe flow", ***Applied Rheology***, 34(1): 20240002, (2024).

[20] Dehouck V., Lateb M., Sacheau J. and Fellouah H., "Application of the blade element momentum theory to design horizontal axis wind turbine blades", ***Journal of Solar Energy Engineering***, 140(1): 014501-1, (2018).

[21] Hasan M.F., Danışmaz M. and Waheed F., "Modern Nanotechnology Application for Generation Highly Efficient Electricity in Save Mode and Much Less Polluting", ***International Journal of Computational and Experimental Science and Engineering***, 8(1): 1-4, (2022).

[22] Yang H., Shen W., Xu H., Hong Z. and Liu C., "Prediction of the wind turbine performance by using BEM with airfoil data extracted from CFD", ***Renewable Energy***, 70: 107-115, (2014).

[23] Selig M.S. and Guglielmo J.J., "High-lift low Reynolds number airfoil design," ***Journal of aircraft***, 34(1): 72-79, (1997).

[24] Chaviaropoulos P. K. and Hansen M.O., "Investigating three-dimensional and rotational effects on wind turbine blades by means of a quasi-3D Navier-Stokes solver", ***Journal of Fluids Engineering***, 122(2): 330-336, (2000).

[25] Filippone A., "Comprehensive analysis of transport aircraft flight performance", ***Progress in Aerospace Sciences***, 44(3): 192-236, (2008).

[26] El-Sayed A.F., "Fundamentals of aircraft and rocket propulsion", London: ***Springer***, (2016).

[27] Ives R., Bassey E. and Hamad F. A., "Investigation of the flow around an aircraft wing of section NACA 2412 utilising ANSYS fluent," ***INCAS Bulletin***, 10(1): 95-104, (2018).

[28] Ahammad R., Hasan M. K., Rahman M. and Chakraborty M., "Performance test of Naca 2412 airfoil," ***In International conference on mechanical engineering and renewable energy***, Chittagong, Bangladesh, 26-29 November (2015).

[29] Quagliarella D., Serani A., Diez M., Pisaroni M., Leyland P., Montagliani L. and Stern F., "Benchmarking uncertainty quantification methods using the NACA 2412 airfoil with geometrical and operational uncertainties," ***In AIAA Aviation 2019 Forum***, 5(3): 3555, (2019).

[30] Chinvorarat S., Watjatrakul B., Nimdum P., Sangpet T. and Vallikul P., "Flight test stall analysis of a light amphibious airplane with NACA 2412 wing airfoil," ***In AIP Conference Proceedings***, 3236(1): 030001, (2024).

[31] He J., Jin X., Xie S., Cao L., Wang Y., Lin Y. and Wang N., "CFD modeling of varying complexity for aerodynamic analysis of H-vertical axis wind turbines", ***Renewable Energy***, 145: 2658-2670, (2020).

[32] Tatlıer M. S. and Baran T., "Structural and CFD analysis of an airfoil subjected to bird strike", ***European Journal of Mechanics-B/Fluids***, 84: 478-486, (2020).

[33] Danışmaz M., Atılğan D. and Karaca F., "Airfoil design and analysis for fixed wing mini-UAVs". ***III. International Congress of Applied Sciences***, Karabagh, Azerbaijan, 07-10 June (2022).

[34] Arik S., Turkmen I. and Oktay T., "Redesign of Morphing UAV for Simultaneous Improvement of Directional Stability and Maximum Lift/Drag Ratio," ***Advances in Electrical & Computer Engineering***, 18(4): 57-62, (2018).

[35] Yeşilbaş E., Özgür B., Ozen E. and Oktay T., "Simultaneous and stochastic design of piston-prop TUAV vertical tail and its autonomous system," ***Aircraft Engineering and Aerospace Technology,*** (2025).

[36] Uzun M. and Oktay T., "Simultaneous UAV having actively sweep angle morphing wing and flight control system design," ***Aircraft Engineering and Aerospace Technology***, 95(7): 1062-1068, (2023).

[37] Oktay, T. and Coban, S., "Simultaneous longitudinal and lateral flight control systems design for both passive and active morphing TUAVs," ***Elektronika ir elektrotechnika***, 23(5): 15-20, (2017).

[38] Oktay T., Arik S., Turkmen I., Uzun M. and Celik, H., "Neural network-based redesign of morphing UAV for simultaneous improvement of roll stability and maximum

lift/drag ratio," ***Aircraft Engineering and Aerospace Technology***, 90(8): 1203-1212, (2018).

[39] Kose O. and Oktay T., "Simultaneous design of morphing hexarotor and autopilot system by using deep neural network and SPSA," ***Aircraft Engineering and Aerospace Technology***, 95(6): 939-949, (2023).

[40] Aslan S., Demirci S., Oktay T. and Yeşilbaş E., "Percentile-based adaptive immune plasma algorithm and its application to engineering optimization," ***Biomimetics***, 8(6): 486, (2023).

[41] Oktay T. and Eraslan Y., "Computational fluid dynamics (CFD) investigation of a quadrotor UAV propeller," ***In International Conference on Energy, Environment and Storage of Energy***, Kayseri, Türkiye, 5-7 June, pp. 1-5, (2020).

[42] Emax GT3526/05 (710KV) motor, "Data Sheet", https://emaxmodel.com/products/gt3526 (Access 10 March 2025).

[43] Evran S. and Yıldır S.Z., "Numerical and Statistical Aerodynamic Performance Analysis of NACA0009 and NACA4415 Airfoils", ***Journal of Polytechnic***, 27(3): 849-856, (2024).

[44] Durmus S. and Ulutas A., "Numerical analysis of NACA 6409 and Eppler 423 airfoils", ***Journal of Polytechnic***, 26(1): 39-47, (2023).

[45] Demir H. and Kaya N., "Multi-objective optimization of an aircraft wing spar section", ***Journal of Polytechnic***, 28(2): 607-616, (2025).

[46] Joshi A. S., Dincer I. and Reddy B. V., "Thermodynamic assessment of photovoltaic systems," ***Solar Energy***, 82(8): 1139-1149, (2009).

[47] Amiri N., Ramirez-Serrano A. and Davies R.J., "Integral backstepping control of an unconventional dual-fan unmanned aerial vehicle," ***Journal of Intelligent & Robotic Systems***, 69: 147-159, (2013).

[48] Taherinezhad M., Ramirez-Serrano A. and Abedini A., "Robust Trajectory-Tracking for a Bi-Copter Drone Using INDI: A Gain Tuning Multi-Objective Approach," ***Robotics***, 11: 86, (2022).

[49] NASA Prediction of Worldwide Energy Resources (POWER), "Data Access Viewer (DAV)", https://power.larc.nasa.gov/data-access-viewer (Access 10 March 2025).

[50] Khan F. A., Islam A., Abbas H., Rasheed S. M. M. H., and Iqbal S., "Computational Analysis of a UAV Drone with Varying Angle of Attacks," ***2nd International Conference on Emerging Trends in Electrical, Control, and Telecommunication Engineering (ETECTE)***, 27-29 November, pp. 1-11, (2023).